MEDIATOR ROLE OF SOME ORGANIC SUBSTANCES IN THE CHARGE TRANSFER ON METAL–ELECTROLYTE INTERFACE

Gheorghe Semenescu
Faculty of Science, University of Pitesti, Romania

Constantin Cioaca, Bogdan Iorga, Gabriela Gughea
Department of Physics, Faculty of Chemistry, University of Bucharest, Regina Elisabeta Avenue, No. 4 – 12, 70346 – Bucharest, Romania

Received 18-06-2001

Abstract

The model "double mixed electric layer" presents an interpretation variant for the cyclic voltammogram and for the polarography mechanism, from the point of view of the interface charge transfer phenomena, mediated by the solution donor-acceptor "impurities". We assign a concrete physical significance for the current steps and peaks, which are characteristic to the cyclic voltammograms.

The paper accredits the idea of the free electron pairs of the nitrogen, from the amino groups, which are involved in charge transfer phenomena, as a support for the electron conduction through bio-structured systems. The discussions are focused on the cyclic voltammograms associated to some electrochemical active organic compounds.

Introduction

In this paper, we try to explain the electrochemical mechanism at the electrode/electrolyte interface in the polarography technique, as a special case, and in the voltammetry technique, as a general case, proceeding from charge transfer phenomena. Some electrolyte solution impurities, which are capable to decrease the activation energy necessary for the electrons transfer process on interface, play an essential role in the interfacial phenomenon, and their effect can be quantitatively evaluated. We suppose that the π-electrons or the unparticipant electron pairs from the functional groups ($-NH_2$ or -SH) of some biological substances can be involved in the charge transfer phenomena. In addition, we pursue the possibilities to measure the dose of the organic "impurities" from solution and the explanation of some electrosynthesis processes as a support for the electron conduction through the bio-structured systems. Finally, we try to classify the phenomena that involve the charge transfer at the interface level: Pt/electrolyte and Hg/electrolyte, in our desire to have a unitary treatment.

Experimental

The measurements have been made with the "Princeton Applied Research" electrochemical system (a potentiostat 273A model and an acquisition system). We used the cyclic voltammetry technique at stationary conditions on Pt-Pt system. A minicell (10 ml) with an Ag/AgCl reference electrode was used. The working electrode and the counter electrode are identically manufactured from two Pt-wires (0.2 cm^2 each electrode).

We tested aerated solutions with different concentration of antipyrine and its derivatives (4-aminoantipyrine, N-2,4dinitrophenyl-4-aminoantipyrine, N-picryl-4aminoantipyrine, N-3,4dioximetylen benzalidin-4aminoantipyrine), aniline and two amino acids (valine and asparagine) in acetonitrile on the electrolytic support like potassium tetraphenylboron, tetraethylamonium chloride or lithium perchlorate. We use antipyrine and its derivatives because these organic substances have painkiller and antipyretic quality.[1]

Results

Figure 1 shows the cyclic voltammogram of the antipyrine in acetonitrile solution in 10^{-2}M tetraphenylboron potassium electrolyte solution. It observes a linear growth of the electrical current from 1.3V to 1.8V potential range.

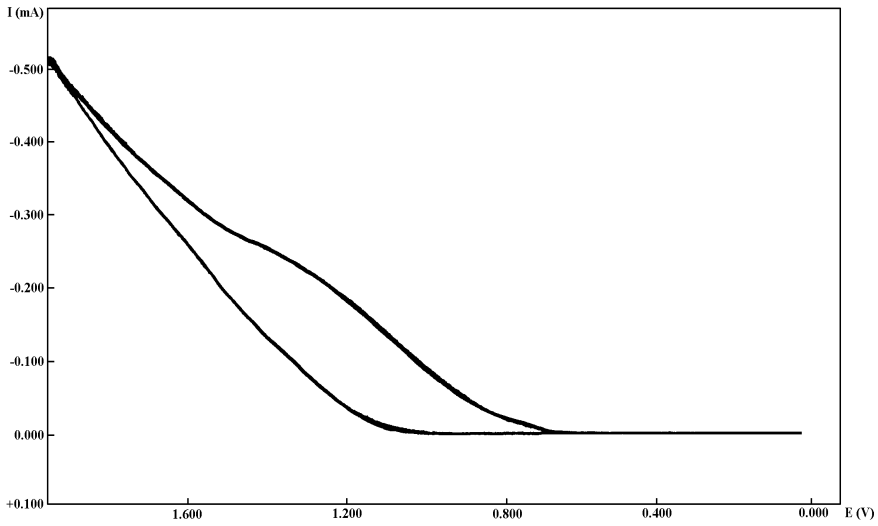

Figure 1. The cyclic voltammogram of antipyrine in acetonitrile solution in 10^{-2} M tetraphenylboron potassium electrolyte drawn for 10 mV/s scanning rate of the potential.

The performed tests in the same conditions of the antipyrine in acetonitrile solutions and its derivatives were disturbed of some depositions of the electrosynthesis products on the electrodes. In 4-aminoantipyrine solutions, one pink electrosynthesis product appears on the anode and perpendicularly on the interelectrodic area. Therefore, the interelectrodic area has a particular status from the viewpoint of structuring of the electrolyte when the electrical circuit is closed.

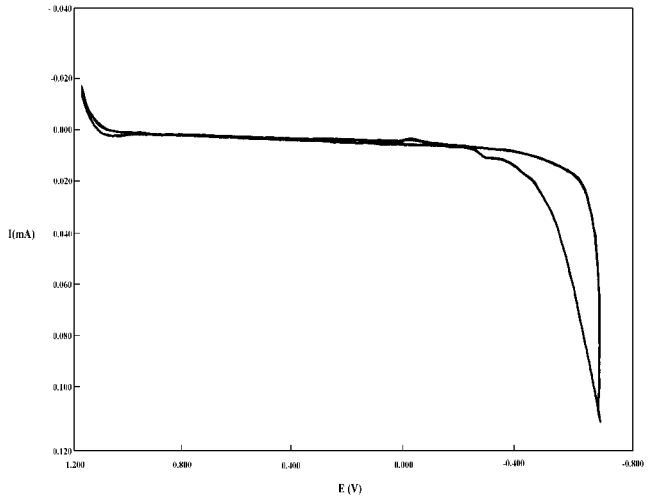

Figure 2. The cyclic voltammogram of antipyrine in acetonitrile solution in 10^{-2} M tetraethylamonium chloride electrolyte drawn for 20 mV/s scanning rate of the potential.

Figure 2 shows the cyclic voltammogram of the antipyrine in acetonitrile solution in 10^{-2}M ammonium tetraethyl chloride.

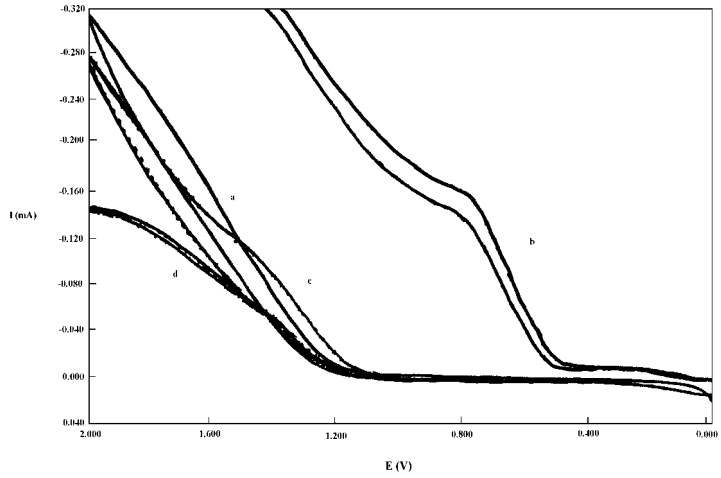

Figure 3. The cyclic voltammogram of the antipyrine (a),4-aminoantipyrine (b), N-2,4-dinitrophenyl-4-aminoantipyrine (c), N-picryl-4-aminoantipyrine (d) in acetonitrile solution in 10^{-2} M tetraethylamonium chloride drawn for 20 mV/s scanning rate of the potential.

In Figure 3 are comparatively plotted the cyclic voltammograms of 10^{-2}M antipyrine in acetonitrile solution (a) and its derivatives as: 4-aminoantipyrine (b), N-2,4dinitrophenyl-4aminoantipyrine (c), N-picryl-4aminoantipyrine (d), in 10^{-2}M ammonium ethyl chloride electrolyte. Similar experiments were performed with 2-mercaptobenzimidazole (a), S-2,4dinitrophenyl-2mercaptobenzimidazole (b) and S-picryl-2mercaptobenzimidazole (c). The adequate cyclic voltammograms are shown in Figure 4.

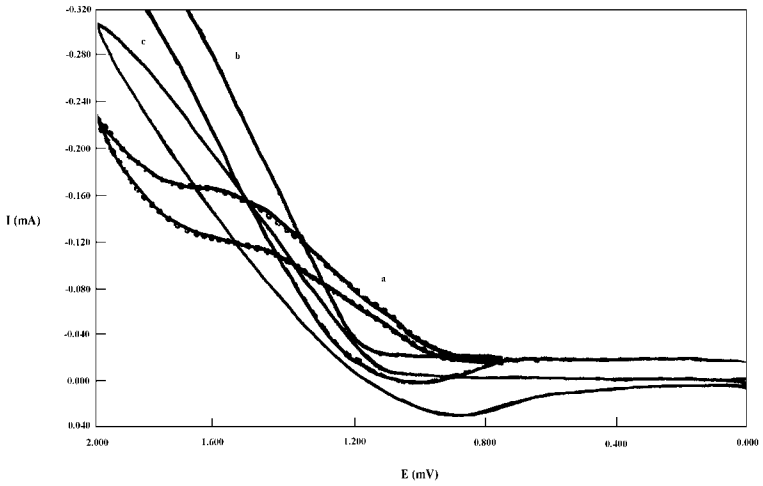

Figure 4. The cyclic voltammogram of 2-mercaptobenztiazol (a), S-2,4 dinitrophenyl-2-mercaptobenztiazol (b), S-picryl-2-mercaptobenztiazol (c).

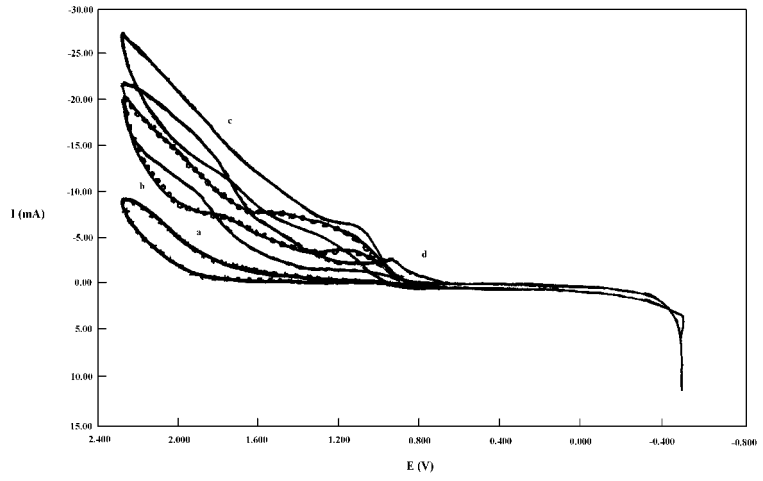

Figure 5. The cyclic voltammogram of 10^{-2}M solutions of N-2,4-dinitrophenyl-4-aminoantipyrine (b), N-picryl-4-aminoantipyrine (c), N-3,4-dioxibenziliden-4-aminoantipyrine (d) in acetonitrile on 10^{-2}M $LiClO_4$ as background electrolyte, drawn for 20 mV/s scanning rate of the potential.

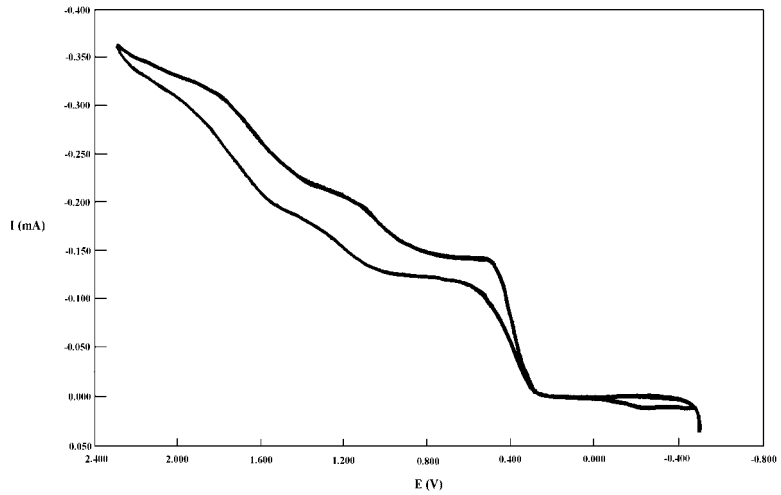

Figure 6. The cyclic voltammogram of 0.125 M 4-aminoantipyrine solution in acetonitrile on 10^{-2} M $LiClO_4$ as background electrolyte.

In Figure 5 are comparatively plotted the cyclic voltammograms of the 4-aminoantipyrine in acetonitrile solution and its derivatives (b, c, d) in 10^{-2}M $LiClO_4$ background electrolyte with the cyclic voltammograms of the $LiClO_4$ electrolyte (a). This voltammograms may be compared with the voltammogram of the 0.125M 4-aminoantipyrine in acetonitrile solution in 10^{-2}M $LiClO_4$ background electrolyte in Figure 6.

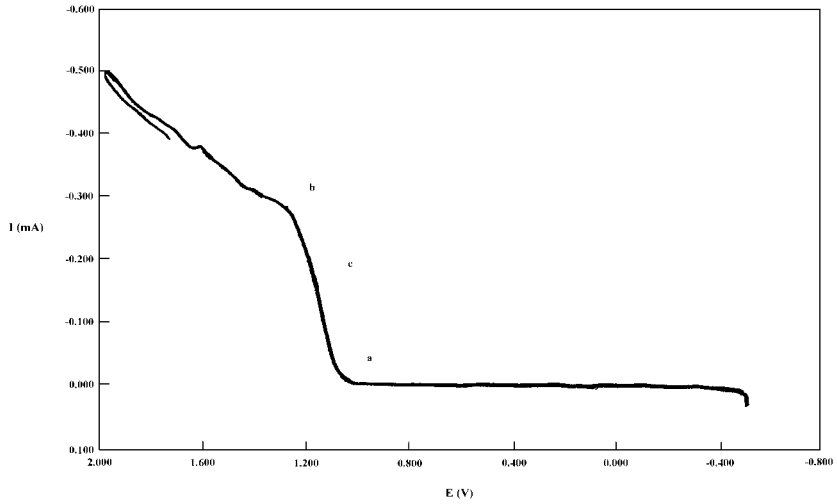

Figure 7. The direct voltammogram drawn on 10^{-2}M $LiClO_4$ as background electrolyte of the antipyrine in acetonitrile solution for 20 mV/s scanning rate of the potential.

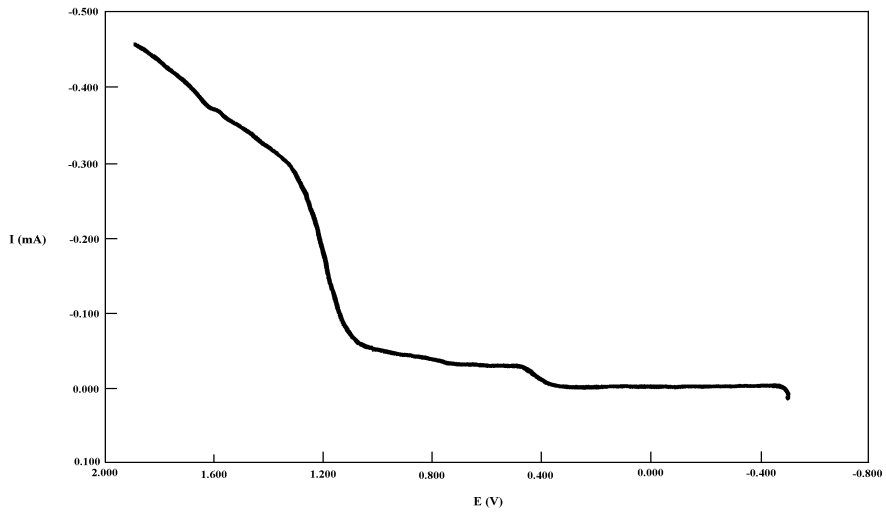

Figure 8. The direct voltammogram drawn on 10^{-2} M $LiClO_4$ as background electrolyte of the mixture of antipyrine and 4-aminoantipyrine in acetonitrile solution for 20 mV/s scanning rate of the potential.

In Figures 7 and 8, the obvious similitude between the cyclic voltammetry and polarography is emphasized. The figures show "the polarographic steps" obtained in the anodic-sense plotted voltammograms for antipyrine solutions and, respectively, mixed 4-aminoantipyrine and antipyrine solutions on Pt-Pt electrodes' system. The background electrolyte is 10^{-2}M $LiClO_4$, and the potential scanning rate is 20mV/s.

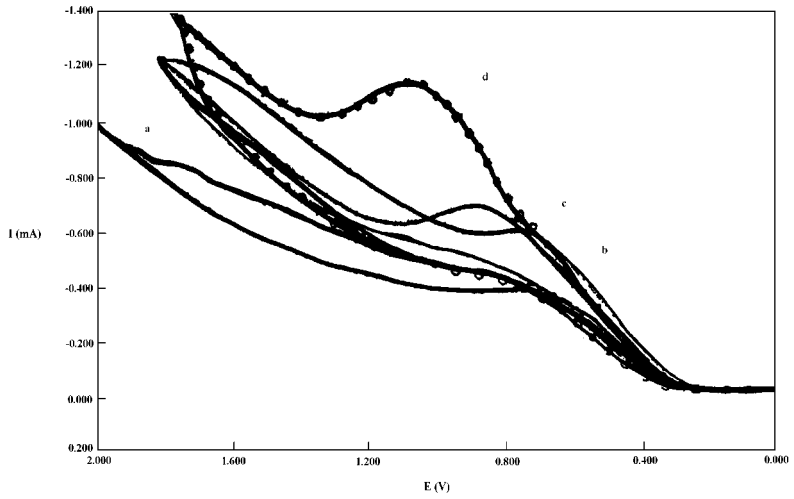

Figure 9. The influence of the scanning rate of the potential on the voltammogram shape drawn in 4-aminoantipyrine in acetonitrile solution on 10^{-2}M $LiClO_4$ as background electrolyte (20 mV/s (a), 100mV/s (b), 300mV/s (c), 1000mV/s (d)).

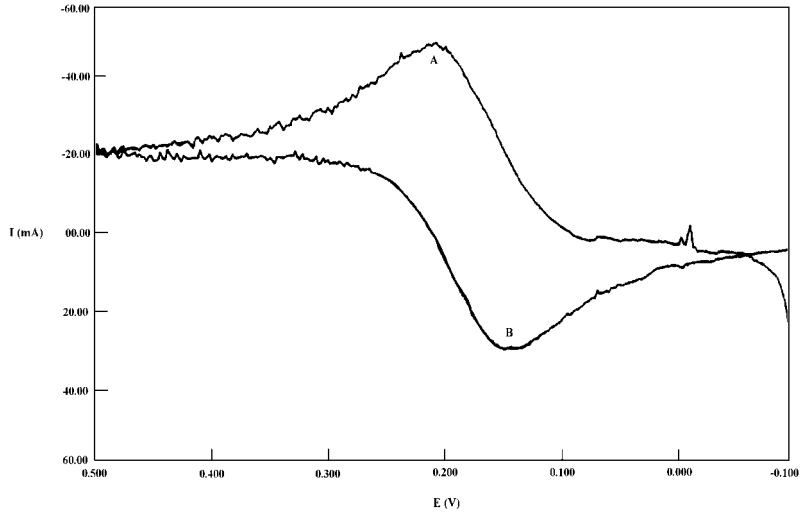

Figure 10. The cyclic voltammogram of a $K_4[Fe(CN)_6]$ solution for Pt/Pt electrodes system in 10^{-1} M KNO_3 as background electrolyte for 5 mV/s scanning rate of the potential.

The influence of the scanning rate upon the recorded electrical current for 4-aminoantipyrine solution is shown in Figure 9. One observes a proportional increase of the electrical current with the square root of the potential scanning rate from 20mV/s (a) to 100mV/s (b), 300mV/s (c) and, respectively, 1000mV/s (d). In the incipient phase, the limiting current is affected by the appearance of a maximum current that increases with the potential scanning rate growth. Such current peaks are a general characteristic of the cyclic voltammograms plotted at high potential scanning rate on systems that involves the interfacial charge transfer phenomena. In Figure 10, it is shown the cyclic voltammogram of a $K_4[Fe(CN)_6]$ aqueous solution in 10^{-1}M KNO_3 electrolyte, plotted for Pt-Pt electrode's system at 5mV/s scanning rate. This voltammogram emphasises a typical reversible electrochemical process. It must be mentioned that the current peaks at 0.5mV/s scanning rate are missing.

The cyclic voltammograms of antipyrine and its derivative's solutions at 20mV/s scanning rate are like those presented in Figure 11.

In Figure 11 the voltammogram of the N-2,4dinitrophenyl-4aminoantipyrine in acetonitrile solution in 10^{-2}M $LiClO_4$ electrolyte is shown. The cyclic voltammograms of valine and asparagine in acetonitrile solutions in 10^{-2}M $LiClO_4$ electrolyte solution emphasize a strong electrochemical activity of the amino acids. This activity is remarked by the decrease of the η_c value. η_c is the critical potential associated with the charge

transfer achieved by $(ClO_4)^{-1}$ anion of the electrolyte. The tests are strongly disturbed by the electrosynthesis products on anode, which are coloured dark-red to black. It is hard to say whether the half-wave potential relative to the Pt anode is real or not, because of the adherent depositions.

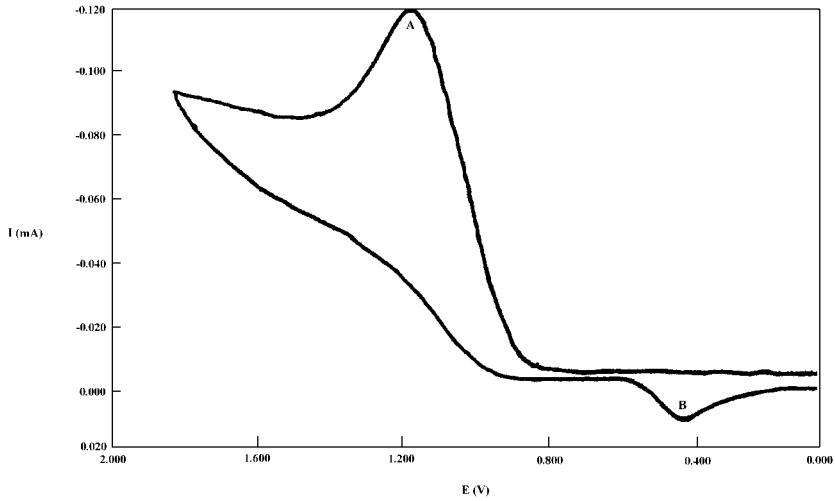

Figure 11. The cyclic voltammogram of 10^{-2} M N-2,4-dinitrophenyl-4-aminoantipyrine in acetonitrile solutions on 10^{-2} M $LiClO_4$ as background electrolyte, drawn for more than 20 mV/s scanning rate of the potential.

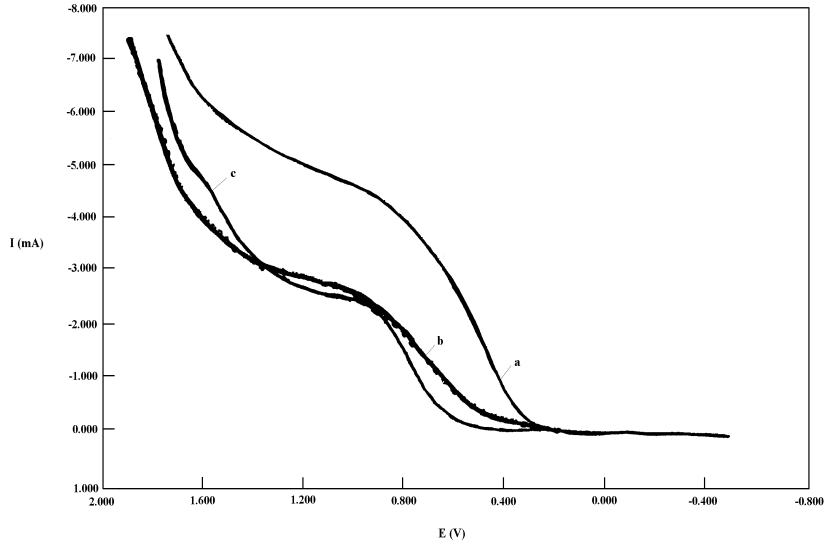

Figure 12. The cyclic voltammogram of the 10^{-2}M $LiClO_4$ solution (a), and of 4-aminoantipyrine for 5. 10^{-4}M (b), and 10^{-2}M (c) concentrations in acetonitrile on 10^{-2}M $LiClO_4$ as background electrolyte.

It was obtained that 4-aminoantipyrine is active only in anodic space using an electrochemical cell with two compartments joined by $LiClO_4$ electrolyte bridge. The cyclic voltammograms of the 4-aminoantipyrine in anodic space, then of the 4-

aminoantipyrine in both spaces, have been obtained. The limiting current, which is a characteristic of the 4-aminoantipyrine, was obtained only in the case in which there was the "impurity" in the anodic space.

The Figure 12 comparatively shows the cyclic voltammograms for different concentrations, $5 \cdot 10^{-4}$M (b) and 10^{-2}M (c), of the 4-aminoantipyrine solution in acetonitrile on $LiClO_4$ electrolyte, with an Ni–Ni electrode system. The addition of the 4-aminoantipyrine determines a decrease of the limiting current.

Discussions

The significant element of the voltammograms in Figures 1, 3, and 4 is the linear current jump which corresponds to a critical value of the applied overpotential, $\eta_{critical}$. This is much lower for the voltammograms (b) in Figure 3 and (a) in Figure 4, and can be associated to an abrupt change of the electric resistance of the circuit in the metal–oxide interface. These differences involve the supposition that, at a threshold value, the N and S unparticipant electron pairs in functional groups $–NH_2$ and –SH would be possibly involved in the interfacial charge transfer phenomena because the platinum can directly adsorb such molecules. Also an adequate polarization of the electrode would be possible to favour these phenomena. The direct adsorption of the organic "impurities" on the electrolyte surface is proportional to their concentration in solution and the electrolyte structuring around the anode is strongly affected in the zones with impurities.

About the behaviour of the substituted derivatives of the 4-aminoantipyrine and 2-mercaptobenztiazole (see Figure 3 and Figure 4), there are two possibilities:

I. The substitute stabilises the unparticipant electron pairs of the $–NH_2$ and –SH groups, which become unavailable for the interfacial charge transfer. The effect is the increasing of the $\eta_{critical}$ value.

II. The steric hindrances determine that the >NH and –S– functional groups become inaccessible for the anode surface to assure the interfacial charge transfer.

In the 4-aminoantipyrine case, it forms in the anode zone a red electrosynthesis soluble product first in the interelectrodic plane, and after the "limit current" is attained, in the opposite space of the interelectrodic plane. Apparently, we have a diffusion of the

coloured product in the bulk solution, but it is possible to have even diffusion in certain directions in the electrolyte. In acid environments (HCl, H_2SO_4), 4-aminoantipyrine becomes weakly red coloured and the acceptor nature of the proton should constitute the cause of the appearance of some species with chromophore groups. Therefore, we cannot exclude the appearance of the same chromophore groups during the charge transfer processes in the anode zone.

A critical potential is obtained for each substance in Figures 5 and 6. In comparison with the voltammogram (b) in Figure 3, here we see a decrease of the critical potential, as an effect of the background electrolyte. The two inorganic ions play an important role in providing the interface charge transfer, in the case of $LiClO_4$ as background electrolyte. Consequently, it is probable that only the reasons of steric order brake this process for other background electrolytes (potassium tetraphenylboron or tetraphenylamonium chloride) having as a result the increase of the $\eta_{critical.}$ The current jump has a linear dependence of the concentration of organic "impurities" in electrolyte in a very broad range: from 1M to 10^{-4}M.

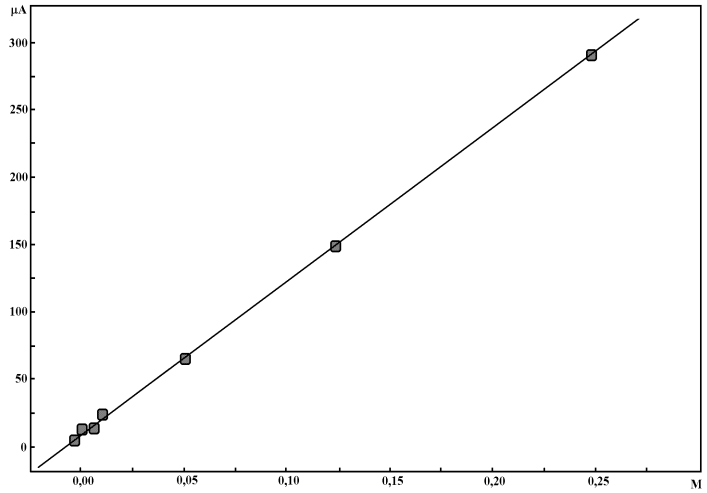

Figure 13. The values of the limiting current as a function of the concentration of a 4-aminoantipyrine solution in acetonitrile at 10^{-2}M $LiClO_4$ as background electrolyte

The graph in Figure 13 shows this for solutions of different 4-aminoantipyrine concentrations. Like in the polarography case, the half-wave potential is a characteristic of the measured substance. The result emphasises the possibility of 4-aminoantipyrine dosing by direct voltammetry with two Pt-electrodes.

From the experiments achieved, we obtain that the background electrolyte play an important role in the electrode process. This can participate as reactant in forming of the electrosynthesis products. The interelectrodic zone has a distinct role in appropriate structuring of the electrolyte when the electric circuit is closed. Also, one concludes the possibility that the unparticipant electron pairs of N, S (eventual of oxygen and phosphorous) from $–NH_2$ and –SH or π-electrons from double bonds to be involved in interface charge transfer phenomena. The unloading of some organic "impurities", with such groups, on Pt-electrode has place for certain critical potential values, which correspond to the substance. The electric current obtained is proportional to the concentration of these in solution (as in case of polarography). These critical potentials are related to the availability for transfer of the different bounded electrons or to the reasons of steric order, which can affect the process of structuring in solution. The critical potentials observed in the voltammograms of these compounds vary in the same way with the energy of the last orbital occupied with electrons and obtained by empirical quantum methods. It is supposed that the 4-aminoantipyrine molecule lies at the interface Pt/electrolyte in the moment of applying an increasing overpotential. As it is known, 4-aminoantipyrine is neutral molecule, with a pronounced amphiphilic character, and liable to the adsorption on solids. For a critical potential $\eta < \eta_{critical}$ ($\eta_{critical}$ is the critical potential assigned to the charge transfer mediated by the ClO_4^- anion in electrolyte-support) the charge transfer mediated by the unparticipant electrons pair of nitrogen in 4-aminoantipyrine molecule is possible. The electron deficit of the formed radical (that became acceptor on the electrode surface) can fast be sets off by the transfer of one electron from the ClO_4^- donor anion. So, we have an increasing of current, which is proportional to the organic "impurity" concentration at the electrolyte/Pt interface.

In Figure 14–I, we show a transverse section through cell in the interelectrodic zone, where we denote by "a" the diameter of the Pt anode and cathode, by "b" the width of the supposed structured zone around the electrodes, by "c" the restructured interelectrodic zone, by "d" the gap in the zone of width "b".

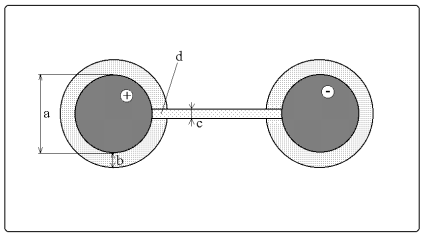

Figure 14-I. Pt-electrolyte interface structure.

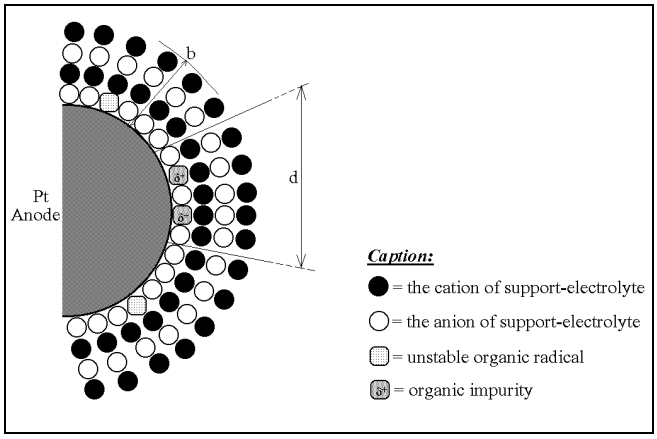

Figure 14-II. Local restructuring of the "b" zone as a result of the "impurities" involved in the charge transfer phenomenon: "b" is the structured zone in accordance with Figure 16; "d" is the structured zone proceeding from the β conduction [8].

In Figure 14–II, we have drawn the possible local restructure of "d" zone under the influence of adsorbed "impurities" involved in the charge transfer phenomenon. For simplicity, we have neglected the solvent molecules in solvation layers.

The high electrical resistance imposed by the electrolyte structuring in zone "b" (Fig.14–I) can be decreased only by the restructuring, even partially, as in zone "d", where the "impurities" which can arrive at interface contribute, by decreasing the activation energy, to the interfacial charge transfer. So, the structure in zone "b" is disturbed at local level with predilection on the minimum interelectrodic distance "c".

The global process of structuring of the electrolyte in the adjacent zone of the electrodes continues in two ways (Fig. 14): the alternative "b" — of a majority and the alternative "d" — local, which in function of the concentration of the "impurities" in solution and of the potential scanning rate, involves two aspects:

a) In the case of a slow variation of the overpotential, comparable with the migration speed of the ions in solution, the adsorbed "impurities" on the Pt-anode are involved step by step in the interfacial charge transfer beginning with the zone in that the distance between electrodes is minimum, and finishing with the other zones, which lie on the remaining active surface. The decrease of the electric resistance is observed in variation of the current as a function of potential I = I (η), in domain (a) of the voltammogram in Figure 7. As long as the overpotential decreases, the process of

structuring of the electrolyte goes on, and therefore electric resistance increases. This fact is observed in domain (b) of the voltammogram. Here stabilisation takes place at the value of "limit" current. In the domain (c), the current varies linearly with the potential. Electric resistance in this domain of intermediate potential varies insignificant with η. For low scanning rate, it eliminates the possibility of spontaneous appearance of some charged currents of the impurities generated by collective adsorption of the ionic species of the background electrolyte.

b) If the scanning rate is high in comparison with the migration speed of ionic species, then will exist more "imperfections" in this process. Therefore, the electric resistance of the electrolyte will decrease in the restructured zone "d" (Fig.14–II), and consequently, the "limit" current will be magnified. We have, in this case, all the superficial "impurities" involved in the charge transfer process, indifferent where they are on the electrode surface.

The collective effort of the anionic donor species of the background electrolyte, which implies the appearance of a "loading current" at the anode, makes the compensation of the electron deficit of the free radicals spontaneously formed at the interface. Consequently, the "limit" current will be temporarily magnified and a peak of the current will appear (for instance, the peak A in Figure 10). The "loading current" increases with the scanning rate, like the "limit current" does. The process is reversible and as long as the superficial "impurities" are reformed, we have a temporary "loading current", as a result of the collective adsorption of the cationic species of the background electrolyte (the peak B in Figure 10).

For neutral organic "impurities", the phenomenon is less probable. The eventual asymmetries can be correlated with the mobility differences of the ions of the background electrolyte. The differences in the magnitude of the peaks A and B can be correlated with the degree of solvatation of these ions.

The viscosity of the environment plays an important role. Thus, one can explain why the addition of gelatine yields smaller polarographic maxima.

The mean lifetime (τ) of the transient organic radical is very short, especially in zone "c" (Figure 14–I) because of the fast unidirectional charge transfer. After the "limit

current" is attained, the increase of the overpotential determines a progressive structuring of the zone "c", and an increase of the electric resistance, R_d.

It follows a fluctuation period of R_d, because the system reacts by different ways to close the electric circuit and the other parallel ways more favourable from the point of view of the electric resistance.

Many of these ways rest unended but they are an efficient source of creating organic radicals with a mean lifetime bigger and a stabiliser like the acetonitrile encourages this. Thus it can appears some electrosynthesis organic products, for instance the red coloured product in the case of 4-aminoantipyrine solution in the outer space of the interelectrodic area.

The previous comments refer to the asymmetric cyclic voltammograms assigned to some electrochemical processes with charge transfer. The reversible electrochemical processes with mass transfer can determine the change of the state of electrode surface. In the case of the reversible electrochemical processes in classical redox systems, like ferro-ferricyanide, the current peaks are symmetrical.[2]

Let's now explain the theoretical considerations, which are in agreement with the previous comments. The solvent plays an important role in phenomena corresponding to the interelectrodic space in closed circuit. Only for the sake of simplicity, we have neglected of the ions solvatation phenomena. Further on, we depict the "double mixed electric layer" structure that we suggest for the electrolyte-electrode interface.[3, 4]

A) Case of the open electric circuit.

For the heterogeneous solid-electrolyte interface, the "double mixed electric layer" model is on basis of the following requisites (see Figure 15): [5]

- The metal-electrolyte interface is heterogeneous at a microscopic scale;
- The oxide surface is hydrated in case of the aqueous solutions;
- The ions in solution are more or less hydrated, in function of their type, electric charge and volume;
- At equilibrium, the anions (A) and cations (C) can be adsorbed on the superficial active centres of the anode;
- The specific adsorbed ions (A_S and C_S) are totally integrated in the solid

surface and modify its superficial structure (in fact, we can consider a new interface, denoted by I in Figure 15 for the specific adsorption of the anions);

- The ions which have an increased chemical affinity for the active superficial centres eliminate the solvent molecule from the hydration layer and interact with the substrate through a single H_2O molecule which is strongly polarised. The plane of centres of these ions is IHP (the Inner Helmholtz Plane) (Figure 15-II);
- The ions, which have a decreased chemical affinity for the active superficial of the substrate, will interact with the electrode surface by means of two dipolar, stabilised H_2O molecules (those from the hydration spheres of the substrate and the ion). The plane of the centres of these ions is OHP (the Outer Helmholtz Plane) (Figure 15-III).[6]

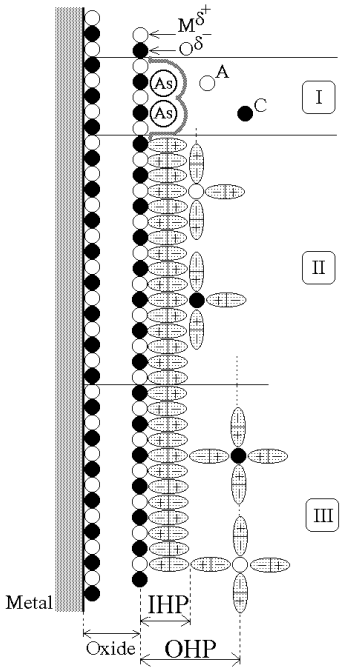

Figure 15. Heterogeneous structure of the metal-oxide/electrolyte interface for double mixed layer of electrode.

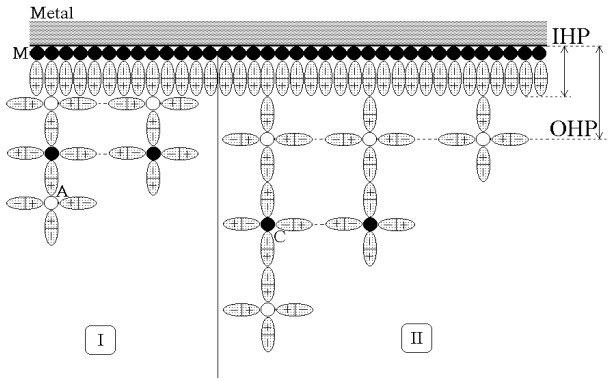

Figure 16. Homogeneous structure of the Hg/electrolyte interface.

If the active superficial acceptor centres of the surface are blocked by the adsorption of the anions A_S, then the surface passes from the mixed-selective state in the cations-selective state (Figure 15-I). In the case of the adsorption of the cations C_S, the phenomena produce conversely. If there is no specific adsorption and the two types of ions are active at the IHP level (Figure 15-II), a mixed electrode potential characterizes

the interface.[7] In this case, one applies Stern's model. If there is specific adsorption and no interactions at IHP level, but only at OHP level, then one applies the Gouy-Chapman model. The same model is applied when in OHP levels the cations and the anions are dominants (Figure 15-III).

For the homogeneous Hg/electrolyte interface and taking into account the molecules in the solvatation sphere, the requisites of this model are as follows:

- There are metallic atoms M which have a great chemical affinity for anions on the homogeneous surface of Hg;
- The Hg surface is hydrated;
- The hydrated ions can interact with the metallic surface.

The adsorbed anions interact with the metallic surface either by the means of a H_2O bimolecular layer that is dipolar stabilised (OHP in Figure 16-II), or through interactions at IHP level (Figure 16-I).

The cations arrive together at the interface form alternating layers, which interact with the anions from IHP or OHP, most probable through dipolar stabilised H_2O bimolecular layers. Passing of the cations from OHP to IHP implies a high activation energy, determined by the dehydration stage, by the strong ionic interaction with the anionic layer from the third layer and by necessity of the layer inversion.

B) Case of the closed electric circuit.

For the solid/electrolyte interface (Figure 15) and for high overpotential, in the adjacent zone of the electrode, appear first the specific interactions between the opposite charged ions mediated by a H_2O molecule and then the interactions between the equally charged ions. The effect consists of the "intermolecular" destruction of the oxide layer.

For the Hg/electrolyte interface (Figure 16), there are two possibilities as a function of the sign of the applied overpotential. The activation of the ions in solution at IHP level requires a high negative overpotential which corresponds to an activation energy needed for the inversion of the water layers and for the inversion of the ionic alternating layers in the adjacent and structured zones of the interface. Only thus the cations can participate in the charge transfer through the interface. The existence of some impurities with a stronger acceptor character in solution could diminish this activation

energy as much more as their concentration is higher. The activation of the ions in solution is made by the putting on a positive small overpotential that corresponds to a small activation energy required only for the inversion and rejection of one of the water molecules, in such a way as the interaction with the Hg to be at IHP level (Fig.16). The same importance has the role of the donor "impurities" in solution which, proportional to their concentration, encourage the charge transfer and the increase of the current to the "limit current" value. Therefore, for the achievement of the interfacial charge transfer it is necessary that the ionic species, with acceptor or donor character, interact with the Hg surface, at least at IHP level.

In the case of dosing the cationic "impurities", the charge transfer processes at IHP level does not suppose the discharge of the metallic cations on the electrode with the forming of the mixture. The mixture is possible to be obtained with increasing overpotential corresponding to the direct interaction of a certain cation with the metallic Hg.

The polarographic phenomenon that permits the dosing of "impurities" (organic or inorganic) in solution is facilitated by the structural interfacial arrangements like those from Figure 16. Because of the result obtained upon the Ni electrode system (Figure12), we think that such image is correct at microscopic level. Thus, the image offered by the "double mixed electrode layer" for the metal-oxide/electrolyte (Fig. 15) is correct. It imposes major restrictions in the phenomenological extrapolation from the Hg/electrolyte interface to that of the solid/electrolyte.

Our paper tries to accredit the idea that common for Hg and Pt, namely the absence of the superficial layer of the heterogeneous oxide is the essence of the polarographic phenomenon. Only in this case the structural arrangement in the Figure 16 is possible. This arrangement is in agreement with the achievement of charge interfacial transfer, in the anode zone and in the cathode zone, too.

Conclusions

In this paper we propose an interpretation mode of the voltammograms and of the polarography mechanism through the viewpoint of the interfacial charge transfer, mediated by the donor–acceptor "impurities" in solution. We assign a physical concrete

significance to the current "peaks", features of the cyclic voltammograms, in accordance with the scanning rate. We believe that in interfacial charge transfer phenomena are involved the pairs of free electrons of the nitrogen and sulphur, as a support of the electronic conduction at bio-structured systems' level.[8] Taking into account the dynamic character of this phenomenon, our interpretation is a phenomenological one.

References

1. S. L. Johansson: *Int. J. Cancer* **1981**, *27*, no. 4, p. 521.
2. J. O. M. Bockris, K. N. Reddy: *Modern Electrochemistry* I; Plenum Press, N.Y., **1970**.
3. L. Oniciu: *Chimie-Fizica. Electrochimie*; Ed. Didactica si Pedagogica, Bucharest, **1974.**
4. L. Radoi, M. Nemes, G. Radovan: *Electrochimie*; Ed. Facla, Timisoara, **1974**.
5. G. Semenescu: *Chem. Rev.*; Bucharest, **1995**, *48*, no. 5.
6. G. Semenescu, C. L. Popescu: *Chem. Rev.*; Bucharest, **1997**, *48*, no. 7.
7. C. Luca, G. Semenescu, A. Andrei: *Chem. Rev.*; Bucharest, **1984**, *29*, no. 1.
8. G. Semenescu, C. Cioaca, B. Iorga: *Acta Chim. Slov*. **2000**, *47*, p. 133-141.

Povzetek

Model dvojne mešane električne plasti predstavlja možno razlago rezultatov ciklične voltametrije in polarografije s stališča fenomenov na fazni meji. Predlagamo razlago za tokovne stopnice in vrhove, ki so značilni za ciklične voltamograme. Razlago smo usmerili na ciklične voltamograme, povezane z elektrokemično aktivnimi organskimi spojinami.